SHEAR BEHAVIOR OF MULTI-STORY REINFORCED CONCRETE WALLS WITH OPENINGS

Rafik Taleb[*] **Supervisor: Susumu KONO**[**]
MEE09187

ABSTRACT

Static loading test was conducted on five 40%-scale specimens in order to evaluate the shear transfer mechanisms of structural walls with and without openings. The experimental variables were the size and location of openings. Failure modes for each specimen and in each direction of loading were identified, and connection between failure modes and the prediction accuracy of the maximum strength by the design equations was made.
From experimental results, shear strength of specimens were estimated using the existing design equations with AIJ and Ono reduction factors. It was shown that the shear strengths of specimens were well estimated combining the shear strength of structural walls without openings estimated by truss and arch mechanism equation and Ono's reduction factor, and it was proved that this method may be applied to structural walls with the opening ratio up to 0.46.
The two-dimensional finite element model constructed well simulates lateral load-drift angle relation and damage distribution for specimens with no or small openings. Both monotonic and cyclic analysis was conducted.

Keywords: Multi-story structural wall, wall with openings, shear strength, strength reduction factor.

1. INTRODUCTION

Multi-story structural walls, which are one of the most important lateral load carrying components in building structures, often have openings for architectural reasons. The number, location and size of the openings affect the stiffness and the strength structural walls with openings; however, it's difficult to evaluate their shear strength and stiffness since the shear resisting mechanism has not been clarified. The Japanese building design standard and guidelines employ strength and stiffness reduction factors computed from the size of openings. This method is simple and convenient but do not reflect the location of openings. The strength reduction factor is given function the opening ratio, η, which expresses the size of the opening. The opening ratio, η, is expressed as:

$$\eta = \max\left\{\sqrt{\frac{h_0 \cdot l_0}{h \cdot l}}, \frac{l_0}{l}, \frac{h_0}{h}\right\} \quad (1)$$

Where h and l is the story height and length, h_0 and l_0 is the opening height and length as shown in Figure 1.

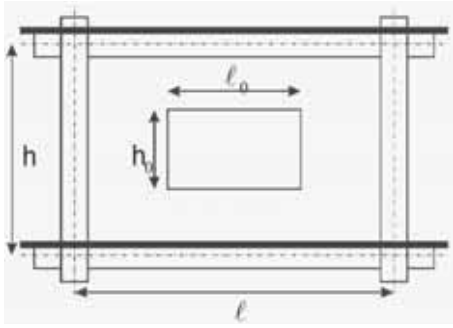

Figure 1. Graphical representation of opening in wall

[*] National Center of Applied Research on Earthquake Engineering (CGS), Algeria.
[**] Assoc. Professor, Department of Architecture and Architectural Engineering, Kyoto University, Japan.

2. EXPERIMENT

2.1 Specimens

Five specimens were a 40% scale model of a lower three-story structural wall system taken from the transverse direction of a typical six-story residential building in Japan. The third story was provided for releasing the confinement caused by the stiff loading beam at the top as shown in Figure 2. Test variables were the size and location of openings. N1 had no openings (η=0.0), S1 had small openings (η=0.3), M1 had medium openings (η=0.34), and L1 and L3 had large openings (η=0.46). The opening location of L1 is eccentric; while for L3 is central. As one of the aims of this study was to clarify the effect of openings on the shear behavior of a structural wall, specimens were designed to fail in shear prior to flexure. Table 1 shows the section size and reinforcement arrangement common to five specimens. Experimental variables are listed in Table 1.
The AIJ shear strength reduction factor due to openings is expressed as follows:

$$r = 1 - \eta \tag{2}$$

AIJ standards (AIJ 1999, AIJ 2010) require that the ultimate shear strength of structural wall with opening shall be computed by multiplying the reduction factor to the shear strength of structural wall without openings. This reduction concept can be applied as long as the opening ratio is less than 0.4 in AIJ standard. This means that the ultimate shear capacity of N1, S1, and M1 can be obtained in this manner but that of L1 and L3 are required to be computed as a frame composed of columns with a standing wall.

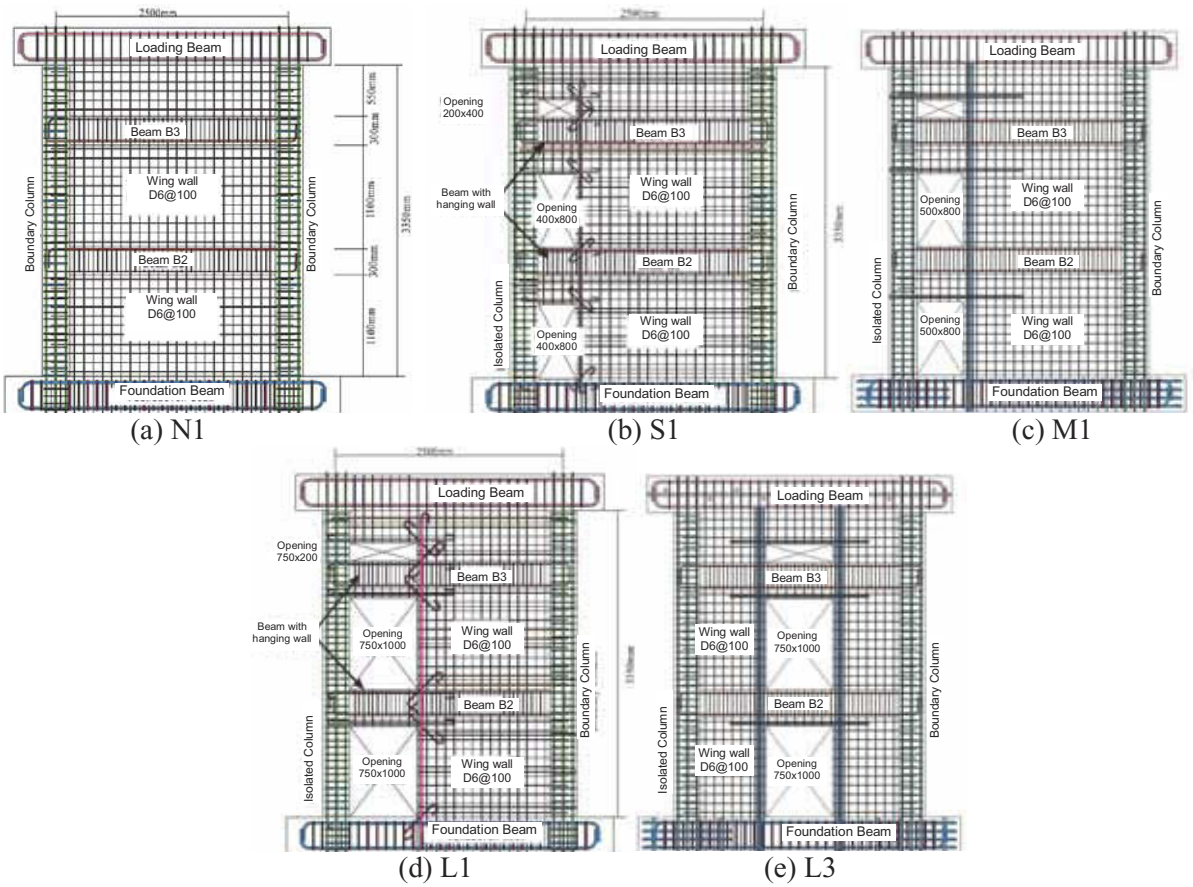

Figure 2. Specimen configurations and reinforcing bar arrangement

Table 1. Reinforcement arrangement around the openings

Member	Section size (mm)	Longitudinal bar		Shear reinforcement	
		Type	Steel ratio	Type	Steel ratio
Boundary column	300×300	8-D19	2.55%	2-φ10@75	0.63%
Beam	200×300	2-D13	0.47%	2-D6@100	0.32%
Wall	t=80	D6@100(Staggered) 0.4% in both vertical and horizontal shear reinforcement			

Table 2. Section size and reinforcing bars in common

	Opening ratio	Reinforcement around the opening		
		Vertical	Horizontal	Diagonal
N1	0	-	-	-
S1	0.30	1-D13	2-D10	1-D13
M1	0.34	3-D13	3-D10	
L1	0.46	1-D16	2-D13	1-D16
L3	0.46	4-D13	4-D10	

2.2 Loading system

Figure 3 shows the loading system. The cyclic reversal lateral load, Q, was applied statically at the midspan of the loading beam through two 2000kN hydraulic jacks. Loading was controlled by displacement at the mid-height of beam B3. The loading protocol was two cycles each at drift angles, R, of ±0.05%, ±0.1%, ±0.25%, ±0.5%, ±0.75% and ±1.0%. During the cyclic horizontal loading, vertical axial loads were also applied by two 1000-kN hydraulic jacks assuming that the specimens are representing a part of the lower three stories of a typical reinforced concrete building with six stories. Hence, the vertical axial load was determined in accordance with the assumed long-term axial loads for a six-storied wall with one span. Thus, 488 kN (244 kN for each jack) was determined as the basic axial load. Moreover, controlling two hydraulic jacks, two vertical axial loads were adjusted to each other so as to keep the apparent shear span ratio ($M/(Qd)$) always 1.0, where M is the flexural moment applied to the base of the wall, Q presents the horizontal load applied to the loading beam, and d is the distance between the center to center spacing between two side columns. (Warashina *et al.*, 2008).

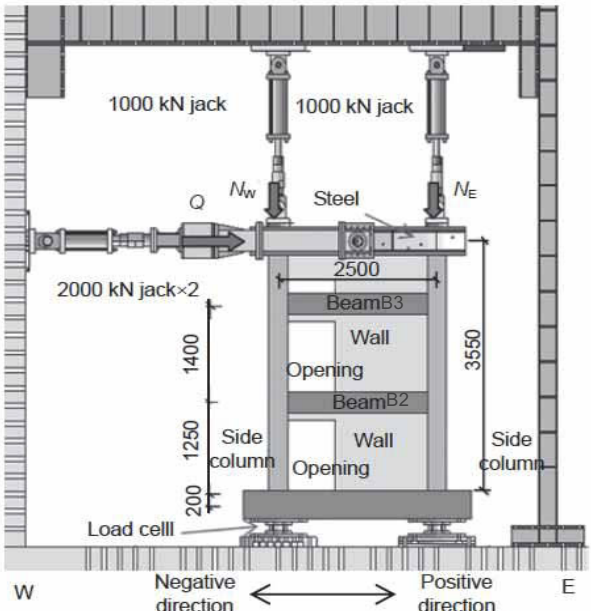

Figure 3. Loading system

2.3. Experimental Results

Figure 4 shows the damage observed in the specimens at R= 0.75%. The shear cracks in the wall panels and the flexural cracks in the tensile column were observed at R=0.05%, and the number of cracks increased until R=0.5%. The load reached the peak between R=0.5% and 0.75% and damage progressed further after the peak load. At this stage, some longitudinal bars of the beams and the reinforcement of the wall were exposed due to the spalling of cover concrete. The buckling of the wall reinforcement in the first story was also observed. At the final loading stage, the shear sliding of the wall occurred and the strength dropped suddenly. Three types of failure mode were observed at the maximum strength, namely, failure due to wide opening of shear cracks developed in wall panels and floor beams, failure due to sliding between shear cracks in wall panels and floor beams and failure due to shear of short span floor beam. Failure modes in all specimens were due to opening or sliding of shear cracks in wall panels and floor beams except for S1 specimen which fail due to shear failure of short span floor beams.

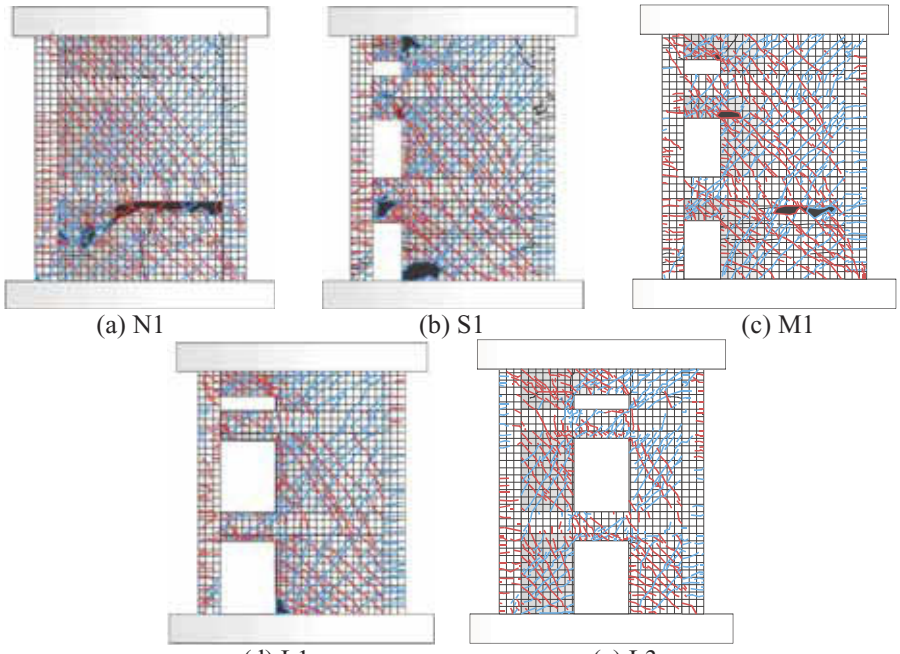

(a) N1 (b) S1 (c) M1

(d) L1 (e) L3

Figure 4. Observed damage at R=0.75%

3. PREDICTION OF SHEAR STRENGTH

The shear strengths are calculated from the design Eq. (3) in AIJ guidelines (2004) based on arch and truss mechanism and the Arakawa design Eq.(4) in JBDPA (2001):

$$V_u = t_w l_{wb} p_s \sigma_{sy} \cot\phi + \tan\theta(1-\beta) t_w l_{wa} \nu \sigma_B / 2 \tag{3}$$

$$Q_{su} = \left[\frac{0.053 p_{te}^{0.23}(18+F_c)}{M/(Q.l)+0.12} + 0.85\sqrt{p_{se}.\sigma_{wy}} + 0.1\sigma_{0e} \right] .b_e.j_e \tag{4}$$

Where t_w is the thickness of the wall panel, hw is the height of the wall, l_{wb} and l_{wa} are the equivalent lengths of the wall panel in the truss mechanism and the arch mechanism respectively, σ_B is the compressive strength of concrete, σ_{sy} is the strength of shear reinforcement in the wall panel, p_s is the shear reinforcement ratio in the wall panel, ϕ is the angle of the compressive strut in truss mechanism. And p_{te} is the equivalent tensile reinforcement ratio, F_c is the concrete compressive strength, b_e is the equivalent wall thickness, p_{se} is the transversal equivalence ratio, σ_{wy} is the yield strength of the transversal reinforcement, σ_{0e} is the axial stress, je is the stress center distance.

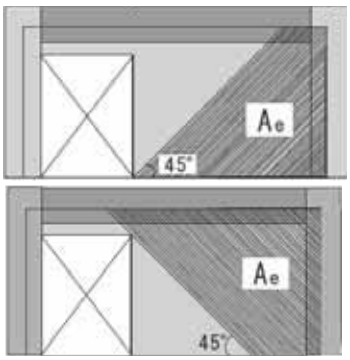

Figure 5. Area of diagonal compression field

The maximum strengths observed in the test, Q_{exp}, are compared with the calculated ultimate strengths, Q_s, as shown in Figure 6 and Figure 7. Both axes are normalized by the flexural strength, Q_f, computed from the approximate design equation based on the flexural theory.

In this study, the AIJ's reduction factors (AIJ 1999, AIJ 2010) based on opening size; while, the Ono's reduction factors, r_u, given by Eq (5) (Ono et al., 1995) is based on the compression field of the concrete panel as shown in Figure 5 were used. For multi-story wall, Ono's reduction factor can be calculated as the minimum of each story (approach 1) or as a one story wall (approach 2).

$$r_u = \sqrt{\sum A_e / hl} \tag{5}$$

A good prediction is given by truss & arch mechanism equation while Arakawa's equation gives conservative prediction. The best prediction is guaranteed by truss & arch mechanism equation with Ono's reduction factor (approach 1).

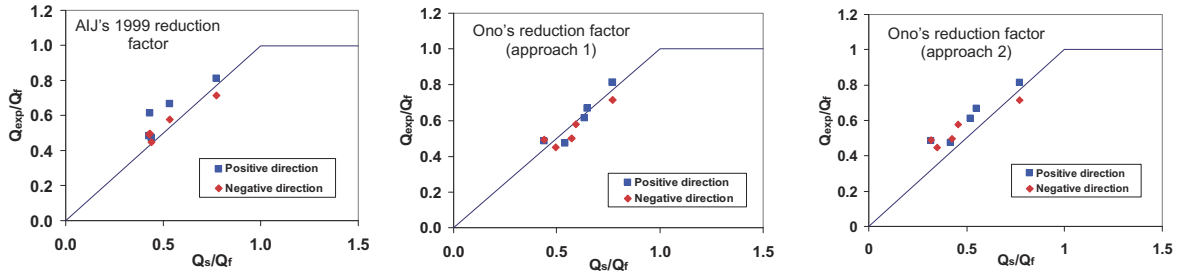

Figure 6. Experimental evaluation of truss and arch design equation

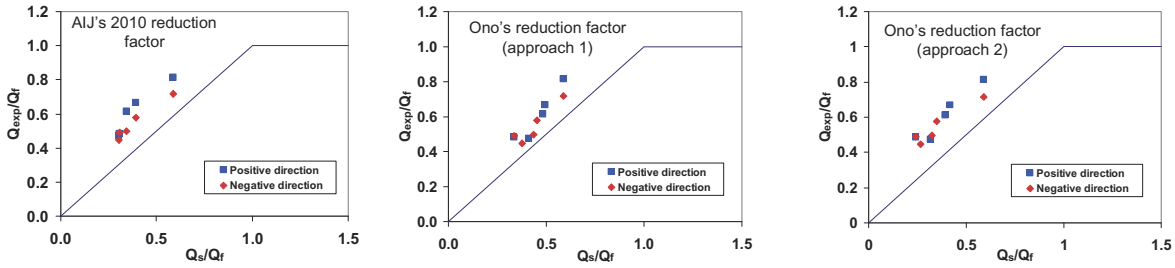

Figure 7. Experimental evaluation of Arakawa design equation

4. FEM ANALYSIS

4.1. Analytical model

In order to simulate the restoring force characteristics and damage, a pushover analysis was carried out using a two-dimensional FEM analysis program. Figure 8 shows the finite element mesh for N1 specimen which employed four-node quadrilateral isoperimetric elements. The element size in the wall panels was 200x200mm. Horizontal and vertical reinforcement was smeared assuming a perfect bond but diagonal reinforcement was neglected. The loading beam and the foundation beam were assumed to be elastic. The concrete constitutive law adopted for cracked concrete is based on the tension stiffening model, the compression model and the shear transfer model (Naganuma *et al.*, 2004). Stress-stain relationship of reinforcement was based on Ciampi model (Naganuma *et al.*, 2004).

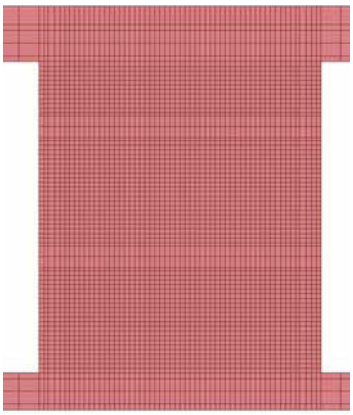

Figure 8. Finite element mesh for N1

4.2. Analysis results

Analytical lateral load-drift angle relations are compared with test results in Figure 9. The analytical results agreed well with the envelops of experimental results for all specimens. The Results illustrate a very good agreement for the maximum strength for all specimens. For the initial stiffness, the analysis was smaller than the experimental value of both positive and negative loading direction for specimens N1, S1 and M1. For specimens L1 and L3, the model slightly overestimates the initial stiffness. For drift angle at the maximum strength, a good agreement is observed for specimens N1 and S1, while for the other specimens, the model tends to underestimate it. This can be explained by the fact that for specimens with large openings, there is certain contribution of flexural behavior.

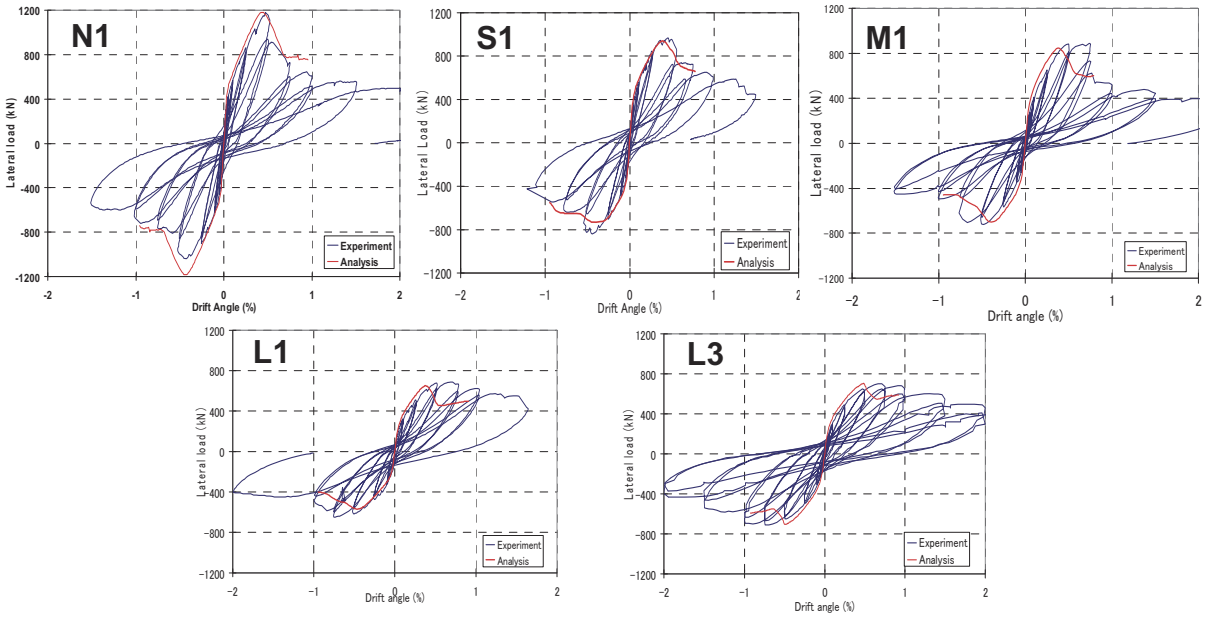

Figure 9. Lateral load–drift angle relationships

5. CONCLUSIONS

The observed damages and failure modes are affected by the openings size and location. Care should be taken to short span beams to avoid their shear failure prior to the wall panels.
It was predicted that shear capacity decreases as the openings stay closer to the center of the wall panel since diagonal compressive strut is difficult to form, especially for large openings. Damage around openings affects also the formation of compressive struts.
The constructed FEM model was verified using experimental results. It was predicted that shear capacity decreases as the openings stay closer to the center of the wall panel since diagonal compressive strut is difficult to form, especially for large openings. Damage around openings affects also the formation of compressive struts. The FEM results show that the shear resisting mechanisms vary depending on the location or size of openings.

6. RECOMMENDATION

It is recommend, using the established FEM model, to perform a parametric study by varying the opening size and location in order to appreciate the accuracy of Ono's shear strength reduction factor more in depth. The main objective of such parametric study is to understand how the opening location affects strength reduction factor.

AKNOWLEDGEMENT

I would like to express my sincere gratitude to my supervisor Pr. S. Kono and to Dr M. Sakashita from Kyoto University for their continuous support, valuable help and guidance during my study.

REFERENCES

Architectural Institute of Japan (AIJ) Standard for RC structures, 1999, Tokyo.
Architectural Institute of Japan (AIJ) Guidelines for RC structures, 2004, Tokyo.
Architectural Institute of Japan (AIJ) Standard for RC structures, 2010, Tokyo. (in Japanese)
Japan Building Disaster Prevention Association, 2001, Tokyo.
Warashina M., Kono S., Sakashita M. and Tanaka H., (2008), 14th WCEE, China.
Naganuma K., Yoneza K., Kurimoto O. and Eto H., (2004), 13th WCEE, Canada.